EXPERIMENTAL CELL RESEARCH 314 (2008) 2846–2854

available at www.sciencedirect.com

ScienceDirect

www.elsevier.com/locate/yexcr

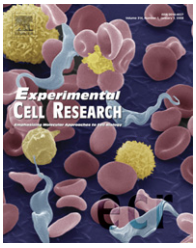

Research Article

Engineering amount of cell–cell contact demonstrates biphasic proliferative regulation through RhoA and the actin cytoskeleton

Darren S. Gray[a], *Wendy F. Liu*[a], *Colette J. Shen*[b], *Kiran Bhadriraju*[b], *Celeste M. Nelson*[a], *Christopher S. Chen*[b,*]

[a]*Department of Biomedical Engineering, Johns Hopkins University School of Medicine, 720 Rutland Avenue, Baltimore, MD 21205, USA*
[b]*Department of Bioengineering, University of Pennsylvania, 210 South 33rd Street, Philadelphia, PA 19104, USA*

ARTICLE INFORMATION

Article Chronology:
Received 23 February 2008
Revised version received 24 June 2008
Accepted 25 June 2008
Available online 9 July 2008

Keywords:
Cell shape
Dielectrophoresis
Endothelial cell
Rho
Tension
Force
Mechanotransduction
VE-cadherin
Cadherin 5

ABSTRACT

Endothelial cell–cell contact via VE-cadherin plays an important role in regulating numerous cell functions, including proliferation. However, using different experimental approaches to manipulate cell–cell contact, investigators have observed both inhibition and stimulation of proliferation depending on the adhesive context. In this study, we used micropatterned wells combined with active positioning of cells by dielectrophoresis in order to investigate whether the number of contacting neighbors affected the proliferative response. Varying cell–cell contact resulted in a biphasic effect on proliferation; one contacting neighbor increased proliferation, while two or more neighboring cells partially inhibited this increase. We also observed that cell–cell contact increased the formation of actin stress fibers, and that expression of dominant negative RhoA (RhoN19) blocked the contact-mediated increase in stress fibers and proliferation. Furthermore, examination of heterotypic pairs of untreated cells in contact with RhoN19-expressing cells revealed that intracellular, but not intercellular, tension is required for the contact-mediated stimulation of proliferation. Moreover, engagement of VE-cadherin with cadherin-coated beads was sufficient to stimulate proliferation in the absence of actual cell–cell contact. In all, these results demonstrate that cell–cell contact signals through VE-cadherin, RhoA, and intracellular tension in the actin cytoskeleton to regulate proliferation.

Introduction

Spatial regulation of proliferation, coordinated by numerous factors in the local microenvironment, is necessary at every stage of multicellular life from embryogenesis through adulthood. Regulators of proliferation include soluble factors [1], cell–ECM interactions [2], cell shape [3,4], mechanical forces [5,6], and cell–cell adhesions [7,8]. In endothelium, cells at wound edges proliferate at greater rates than those in the interior of the monolayer [9]. Similarly, cells comprising the tips of sprouts during angiogenesis proliferate while their neighbors remain quiescent [10]. In these spatially regulated cases the degree of cell–cell contact correlates with, and may be a direct regulator of, changes in proliferation. While previous studies have demonstrated a role for cell–cell contact in regulating proliferation, the mechanisms of such control appear to be complex, and have not been fully elucidated [11,12].

Most previous studies of cell–cell adhesions in endothelial cells have concluded that their formation inhibits proliferation [7,11,13–16]. The classical method which lead to the widespread belief that cell–cell contact decreases proliferation was to compare proliferation rates in sparse cells, having few or no cell–cell contacts, to

* *Corresponding author.*
E-mail address: chrischen@seas.upenn.edu (C.S. Chen).

0014-4827/$ – see front matter © 2008 Elsevier Inc. All rights reserved.
doi:10.1016/j.yexcr.2008.06.023

proliferation rates in cells contacting multiple neighbors within densely crowded monolayers [1]. This phenomenon, known as contact-dependent inhibition of cell proliferation, has been shown to require VE-cadherin, since cadherin-null cells fail to fully arrest proliferation at confluence [7,11,13–15]. However, in these early studies, a high degree of cell–cell contact inhibited proliferation under conditions where cell adhesion and spreading on the underlying extracellular matrix was restricted by virtue of cell crowding. Since cell spreading itself is known to affect proliferation [4,17], our group studied the proliferative effect of VE-cadherin using a new strategy, based on culturing cells in microfabricated wells, in order to separate the independent roles of cell–cell and cell–matrix adhesion [8,18]. Using this system, contact with a single neighboring cell unexpectedly increased proliferation under conditions of constant spreading, and this effect required VE-cadherin. While our previous studies suggested that cell–cell contact arrested proliferation in monolayers because contact decreased cell spreading on ECM, another possibility is that the small amount of cell–cell contact in our two-cell patterns stimulates proliferation while the large amount of contact in monolayers arrests proliferation.

Here, we used a novel micropatterning approach to investigate whether the number of contacting neighbors can differentially regulate endothelial proliferation. While the microfabricated wells used previously facilitated the formation of pairs of cells, it was difficult to form groups of three or more cells with specified arrangements of cell–cell contacts. To overcome this limitation we developed a method which uses dielectrophoretic traps to actively and simultaneously position the cells onto a substrate [19]. Several studies have demonstrated that, under appropriate conditions, dielectrophoresis (DEP) can in fact be used to harmlessly manipulate endothelial cells and a variety of other cell types [19–23]. This active positioning technique enables the patterning of cells in configurations that are otherwise unobtainable by passive micropatterning techniques in which the pattern fidelity is determined randomly.

In the current study, we set out to discern the effect of cell–cell contact on proliferation in a relatively complex yet well-controlled environment. Modulation of cell–cell contact from zero to three uniformly spread neighbors demonstrated a biphasic relationship between cell–cell contact and proliferation. While one neighbor increased proliferation, two or three neighbors diminished this increase. We then investigated the hypothesis that the pathway responsible for these proliferative effects involves a VE-cadherin-derived signal mediated by the actin cytoskeleton. This study demonstrates that quantitative changes in cell–cell contact modulate proliferation through RhoA signaling and intracellular tension, and highlights a novel control mechanism by which cells autoregulate their responses as a function of subtle changes in multicellular organization.

Materials and methods

Cell culture and reagents

Bovine pulmonary arterial endothelial cells (BPAECs, VEC Technologies, Rensselaer, NY) were cultured in a standard growth media containing Dulbecco's Modified Eagle Medium supplemented with 10% calf serum, 100 U/mL penicillin, and 100 μg/mL streptomycin (Invitrogen). Prior to experiments using dielectrophoresis, cells were detached using 0.25% trypsin and 1 mM ethylenediaminetetraacetic acid in PBS, rinsed with 22 μg/mL Soybean trypsin inhibitor (Invitrogen) in growth media, pelleted by centrifugation at 240 *g* for 4 min, resuspended in 3 mL of 300 mOsm sucrose with 1% calf serum (sucrose media), vacuum degassed, and pulled into syringes already containing 1 mL of 10% CO_2/air. After dielectrophoresis, sucrose media was replaced with growth media. Cells plated on passive substrates were resuspended in growth media immediately after trypsinization.

Patterning cells onto substrates

Groups of one to two cells were patterned without the assistance of dielectrophoresis as described previously [8,18]. Briefly, agarose was perfused under a polydimethylsiloxane (PDMS) mold containing raised regions of various geometries, and sealed over a glass surface. Where the raised regions sealed against the glass, fluid was prevented from flowing between the PDMS and the glass, and thus these areas remained free of agarose. Upon agarose curing, and peeling the mold off the glass substrate, the agarose remained adhered to the glass. Substrates were then immersed in 10 μg/mL human fibronectin (Collaborative Biomedical Products), which adsorbed only to the agarose-free areas. Cells were then seeded onto the substrates, attaching only in the regions coated with fibronectin. For maximum patterning efficiency, cells were seeded ~10^4 cells/cm^2 in growth media, and rinsed with fresh growth media at 2 h after seeding.

Substrates used to pattern groups of one to four cells via dielectrophoresis were embedded with arrays of 3 μm electrodes, designed to trap one cell per electrode, as previously described [19]. To increase adhesion between the substrates and the agarose, substrates were coated with an amino functionality using 3-(Aminopropyl)trimethoxysilane (APTES, Aldrich Chemical). Briefly, after treatment with an air plasma (Plasma Prep II, SPI supplies, West Chester, PA) for ~1 min, substrates were placed in a desiccator also containing a drop of APTES on a microscope slide. The desiccator was evacuated and placed at 60 °C overnight. To align the agarose layer with the electrodes, a PDMS mold (see above) was adhered to a glass backing to prevent feature distortion and to facilitate alignment using a mask aligner (Karl Suss, Munich, Germany). Agarose was then wicked under the aligned mold as described above.

To pattern cells using dielectrophoresis (DEP), a parallel plate flow chamber (Fig. S1, S2), similar to that described previously [19,24], was used to introduce cells to the substrates, remove extra cells, and provide a constant supply of fresh media. The floor of the chamber consists of the substrate itself, and a silicone gasket forms the walls of the 160 μm high, 15 mm wide chamber. The electrical signal (5 V, 2 MHz) used to operate the traps was applied to substrates and the counter electrode using a battery operated dual signal generator. The chamber was sterilized with ethanol and dried before each use. As previously described [19], sucrose media containing ~10^6 cells/mL was introduced into the system from 3 mL syringes via rubber tubing. After cells began to flow over the substrate, as monitored by a microscope, the electrodes were energized and began to trap cells. A flowrate of ~50 μL/min for 5 min allowed single and multiple cells to be trapped at the electrodes. A 4-way valve was then used to switch between cells and cell-free media without introducing bubbles into the system.

Flow was increased to ~150 μL/min for 5 min in order to remove the extra cells, leaving in general one cell at each electrode. The flow chamber was then placed at 37 °C with a flowrate of 20 μL/min. After 20 min at 37 °C, the cells had attached to the substrate, which was then gently removed from the flow chamber and aseptically placed in standard culture media (growth media) in a tissue culture incubator.

Immunofluorescence and imaging

Cells were fixed and stained at 24 h after seeding. For the detection of actin, cells were fixed in 4% paraformaldehyde in PBS, blocked and permeablized with 0.2% BSA and 0.2% Triton X-100 in PBS (IF Buffer), and incubated in 0.1 μg/mL TRITC-phalloidin (Sigma) in IF Buffer. For the detection of β-catenin, paraformaldehyde-fixed cells were permeabilized in 0.2% Triton X-100 in PBS, blocked in 33% goat serum in PBS, incubated in 2 μg/mL anti-β-catenin antibody (Santa Cruz Biotechnologies, Santa Cruz, CA), and visualized with Alexa 488- or 594-conjugated secondary antibodies (Molecular Probes). Images of fluorescent stains, as well as non-fluorescence images, were recorded using an inverted microscope (Nikon) and an Orca CCD camera (Hamamatsu, Hamamatsu City, Japan).

Measurement of proliferation

To determine entry into S phase, a commercial assay (Amersham) was used to detect the percentage of cells incorporating 5-bromo-2′-deoxyuridine (BrdU). Cells were synchronized in G_0 by holding cultures at full confluence, as judged by cells attaining a "cobblestone" morphology, for 2 days prior to experiments. BrdU was added to the culture media 2 h after the start of experiments, which ran for 29 h. Cells were then fixed and stained according to a protocol similar to the manufacturer's. Our protocol deviated in that, instead of using an acid/alcohol treatment to fix and permeabilize cells, we used 5% acetic acid alone, followed by permeabilization with 0.2% Triton X-100 (Sigma). The DNA-binding dye Hoechst (Molecular Probes) was used at 1 μg/mL as a counterstain. BrdU incorporation was visualized and scored using an epifluorescence microscope (Nikon). For all proliferation conditions, at least 400 cells were counted across at least three independent experiments.

Statistical significance in trials using dielectrophoresis was determined using Paired Student's *t*-test, because all cells for a given trial were cultured on one substrate. In all other cases, cells were cultured on multiple substrates, and statistical significance was determined using Student's *t*-test.

Construction and use of recombinant adenoviruses

A recombinant adenovirus encoding either GFP, or RhoN19 in tandem with GFP, was prepared using a commercially available kit (AdEasy XL, Stratagene), according to the manufacturer's instructions as previously described. Adenoviral infection was monitored by GFP fluorescence, and adenoviral particles were obtained by cell extraction after 7–10 days. The virus was further amplified, and purified by CsCl gradient centrifugation. Stocks of ~10^{10} infectious particles/mL were retained for use in experiments. The virus was titrated by infecting BPAECs with serially diluted stocks and counting GFP-expressing cells at 24 h. To infect BPAECs for subsequent experiments, cells were exposed to culture media containing 10–100 viral particles/cell for 3 h. Cells were then washed, trypsinized and patterned onto substrates. At 24 h after patterning, >95% of cells were infected. Although RhoN19 expressing cells were co-transfected with GFP, resulting fluorescence levels varied. Therefore, CellTracker Green dye (Molecular Probes) was used to unambiguously label transfected cells, facilitating mixed cell experiments.

Western blot

Cells were washed twice in PBS and lysed in SDS-PAGE sample buffer. Proteins in the lysates were separated by denaturing SDS-PAGE on 4–20% polyacrylamide gradient gels, electroblotted onto PVDF, blocked with nonfat milk in TBS, and immunoblotted with primary antibodies specific to dual-phosphorylated myosin light chain (Cell Signaling Technology, Beverly, MA) or total myosin light chain (Sigma). A VersaDoc Imaging System (Bio-Rad) was used to detect band intensity using horseradish peroxidase-conjugated secondary antibodies (Amersham) and SuperSignal West Dura (Pierce) as a chemiluminescent substrate.

Cadherin-coated beads

Recombinant protein composed of human VE-cadherin fused to the Fc domain of IgG (hVE-Fc, R&D Systems) was used at 100 μg/mL in 0.1% BSA for binding to protein A-coated latex beads (Bangs Laboratories). These beads, with a mean diameter of 5.5 μm, were applied to cells 2 h after seeding, and cells were fixed and analyzed for proliferation as described above.

Results

Dielectrophoresis-mediated construction of multicellular aggregates

To determine the proliferative effects of varying the number of neighboring endothelial cells forming cell–cell contacts, we first developed a method to easily control the exact number of cells confined within multicellular aggregates, by combining two techniques developed by our group. The first method uses micropatterned wells to control the spreading and cell–cell contacts of neighboring cells [8,18]. The second method uses harmless electrical forces to position individual cells at specific locations on a surface, with cell locations defined by the positions of electrodes embedded within the culture substrate [19]. We combined the two methods by fabricating substrates containing both the embedded electrodes and the microwells. Here, the number and positions of the electrodes determine the number and organization of the cells on the surface, while the geometry of the microwells constrains how cells can make contacts with each other. In practice, cells are introduced to the substrate by fluid flow (Figs. 1A, B). Cells are then allowed to attach and spread, at which time the electrodes are turned off (Fig. 1C).

To generate groups of cells having zero to three neighbors, we used four different shapes of wells (Figs. 2A–D). A triangle-like well was used to study cells without contacts, while multi-lobed wells were used to study cells with various amounts of cell–cell contacts

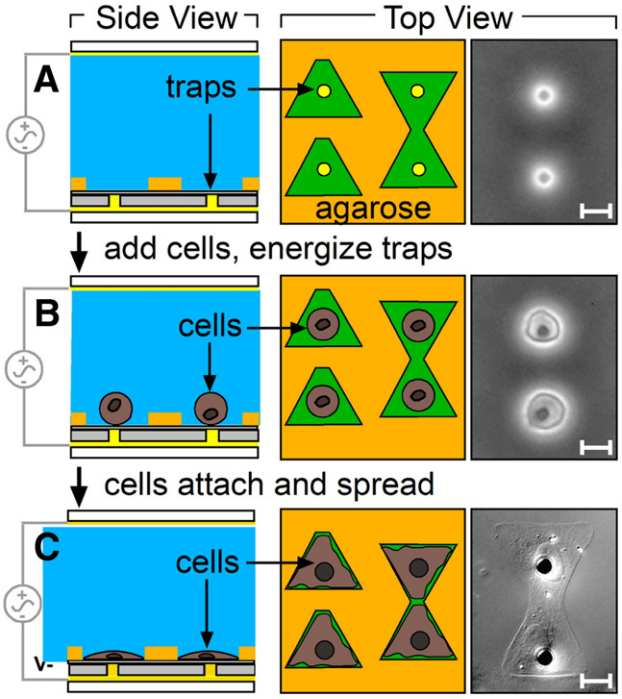

Fig. 1 – Schematic of process used to pattern cells. Each stage in the process is illustrated in top and side views. (A) Flow chamber used to position cells using dielectrophoresis. The Plexiglas lid of the chamber (white) is coated with a thin flat gold electrode (yellow). The floor of the chamber is made by a removable substrate, embedded with gold trapping electrodes (yellow) and covered with agarose (orange) wells patterned in registration with the electrodes. The bases of the agarose wells are coated in cell-adhesive fibronectin (green, top view only). Because the gold on the lid and the substrate is thin enough to be transparent, standard microscopy can be used to visualize the inside of the chamber. (B) Cells are introduced to the chamber by fluid flow, and one cell is drawn to each electrically active trap. Excess cells are removed from the chamber by fluid flow. (C) Cells adhere and spread on fibronectin-coated regions surrounding traps. The non-adhesive agarose barriers define cell shape and cell–cell contact. After cells have adhered, the substrate can be aseptically removed from the chamber and placed in standard culture conditions. Photomicrographs of the top view are either phase contrast (A, B) or differential interference contrast (DIC) (C). Scale bars are 10 μm.

(Figs. 2B–D). One or more electrical traps were placed under the base of each well. Because a single cell was held at each trap, the number and locations of the cells were determined by the number and locations of the traps. The cells would then adhere to the fibronectin coating the base of the well and spread to the confines of non-adhesive agarose, which formed the walls of the well. To generate groups of two, three, or four cells having one, two, or three neighbors, we generated wells with multiple juxtaposed triangle-like regions, separated by narrow constrictions (Figs. 2B–E). After one cell was trapped in each triangular region by means of an electrical trap, the cells adhered and spread to the confines of their respective regions. The constrictions forming the borders between multiple regions prevented cells from migrating into neighboring areas while still allowing the cells to form cell–cell contact at each constriction. For pairs of cells, we used wells made of two triangular regions and resembling a bowtie or hourglass (Fig. 2B). For groups of three (Fig. 2C) or four (Fig. 2D) cells, we surrounded a central cell with two or three neighbors, respectively. By using these groups of juxtaposed triangles, cells would spread and flatten to the same degree in each pattern, while the number of neighboring triangular regions determined the amount of cell–cell contact that could be made. Each triangle had an area of 750 μm^2, thus determining the projected area of cell spreading.

Groups of one or two cells, having zero or one neighbors, respectively, could also be formed without activating the electrical traps. Cells that were seeded onto substrates with wells containing a single triangular region or bowtie-shaped wells containing two regions would often fall into the desired configuration (one cell per triangular region of the well) by random chance. However, groups of three or more cells rarely formed spontaneously by this method, necessitating the use of active electrical patterning.

Proliferation responds biphasically to cell–cell contact

To determine the effect of the number of cell–cell contacts on cell proliferation, endothelial cells were G_0-syncronized by holding them at confluence for 48 h, and then replated, by dielectrophoresis (DEP) when necessary, into wells allowing contact with zero to three cells. Proliferation was assessed by the incorporation of 5-bromo-2′-deoxyuridine (BrdU) at 29 h after plating. Consistent with previous studies [8,18], cells with a single neighbor proliferated at roughly twice the rate of cells with no contacts that were spread to the same degree (Figs. 2F–H). In the current study, three different multicellular aggregates, having two to four cells, all contained cells along their peripheries that had one contact. For example, cells on either end in a threesome made contact with only one neighbor (the central cell in their group). Proliferation in these cells with a single neighbor was similar regardless of the number of other cells in their group.

Upon further increasing the number of contacting cells to two or three, as seen in the center of the “boomerang” (Fig. 2C) or “propeller” (Fig. 2D) configurations, proliferation decreased rather than increased relative to cells with a single neighbor (Figs. 2F–H). This small but statistically significant decrease indicates that cell–cell contact biphasically increases and then decreases proliferation. Depending on the amount of cell–cell contact present, proliferation can be positively or negatively regulated.

Proliferation change depends on cytoskeletal tension and RhoA signaling

Previous results have indicated that tension within the actin cytoskeleton may be involved in the proliferative response to cell–cell contact [8]. To further investigate this possibility, we examined the degree of actin stress fiber formation in cells with zero to three neighbors (Figs. 3A–D). G_0-syncronized cells were positioned in groups of one to four cells for 24 h, and then fixed and stained for actin stress fibers with a fluorescently labeled phalloidin. Single cells cultured in triangular wells showed relatively intense staining of F-actin at the cortex, and few stress fibers in the interior of the cell (Fig. 3A). In contrast, cells in groups of two to four showed less cortical F-actin distribution and significantly higher stress fiber formation (Figs. 3B–D). These stress fibers

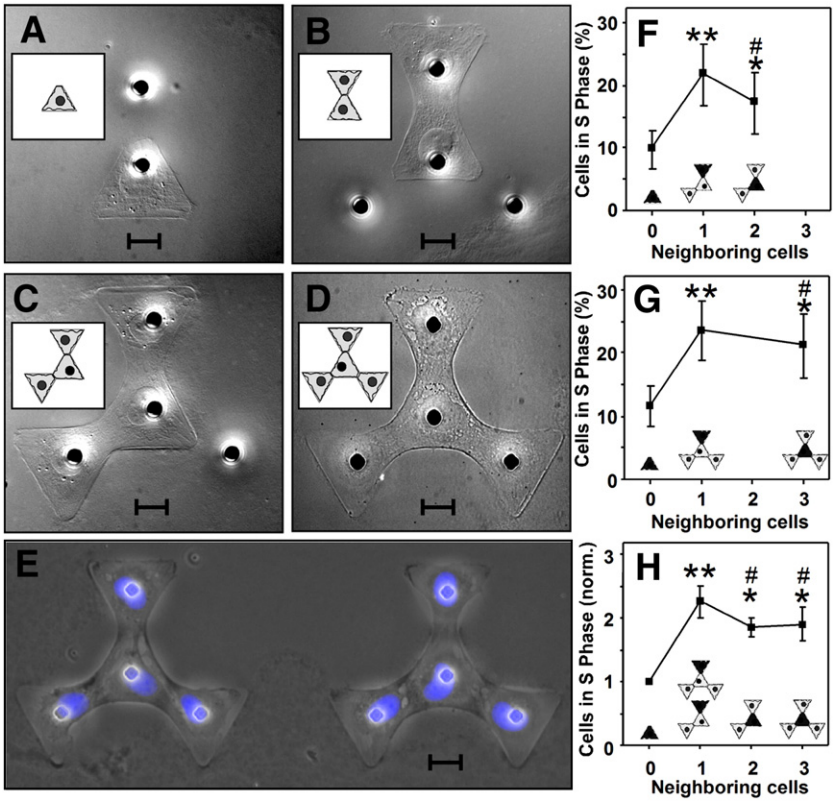

Fig. 2 – Relationship between proliferation and amount of cell–cell contact. (A–D) DIC micrographs and illustrations (insets) of groups of one (A), two (B), three (C), or four (D) BPAECs. These wells are referred to in the text by the shapes they resemble: a triangle (A), a bowtie (B), a boomerang (C), and a propeller (D). The cells are patterned using dielectrophoresis and constrained with agarose wells such that, within the groups, cells contact zero to three neighbors. (E) Phase contrast image of groups of four cells, overlaid with corresponding nuclear stain (blue) used to verify correct cell number for all experiments. (F) Graph of BrdU incorporation with one- and three-cell groups (having zero, one, or two neighbors). (G) Graph of BrdU incorporation with one- and four-cell groups (having zero, one, or three neighbors). (H) Combined graph of BrdU incorporation in cells with zero to three neighbors. To correct for drift in baseline proliferation between experiments, the data in (H) are normalized to the value for cells with no neighbors. In (F–H), shaded cells in illustrations correspond to cell(s) analyzed for the corresponding data point. Error bars are standard error, with (*) $p<0.05$ versus zero neighbors, (**) $p<0.001$ versus zero neighbors, and (#) $p<0.05$ versus one neighbor by paired *t*-test. Scale bars are 10 μm.

typically appeared to form continuous links across cell–cell junctions. Furthermore, cells with one or more neighbors appeared to ruffle and attempt to send processes beyond the agarose walls of the confining wells (Figs. 3B–D). Cells without contacts appeared to be relatively quiescent, having few if any peripheral ruffles (Fig. 3A). The increased membrane ruffling and stress fiber formation correlated with the observed increase in proliferation and suggested an activation of the Rho GTPases. We did not see any clear differences in stress fiber formation or ruffling in cells with one neighbor versus cells with multiple neighbors, suggesting that the down-regulation in proliferation seen with increasing numbers of cell contacts may be unrelated to the observed changes in the actin cytoskeleton.

Based on these observations, we investigated whether RhoA signaling was directly involved in the cell–cell contact-induced proliferative response. We transduced G_0-syncronized cells with a recombinant adenovirus expressing dominant negative RhoA (RhoN19). Expression of bicistronic GFP confirmed a high efficiency of transduction (>95%) in our endothelial cells. We observed a decrease in myosin light chain (MLC) phosphorylation by western blot (Fig. 3E), confirming functional activity of the dominant negative Rho. Infection with Ad-RhoN19 also specifically prevented the increase in stress fibers due to cell–cell contacts, without significantly affecting the organization of F-actin in cells without contacts (Fig. 3F–I). Both single and paired cells transduced with a control adenovirus expressing GFP only (Ad-GFP) exhibited stress fiber distributions similar to corresponding untreated cells (not shown).

To determine whether RhoA signaling affected cell proliferation, we plated G_0-synchronized cells into triangular and bowtie-shaped wells, and measured proliferation rates. Abrogation of RhoA activity specifically reduced the cell–cell contact-dependent increase in proliferation without significantly affecting the proliferation rate in single cells (Fig. 3J). Both single and paired control cells infected with Ad-GFP had proliferation rates similar to corresponding untreated cells (not shown). Together, these findings suggest that RhoA activity was necessary for the cell–cell contact-mediated increase in proliferation.

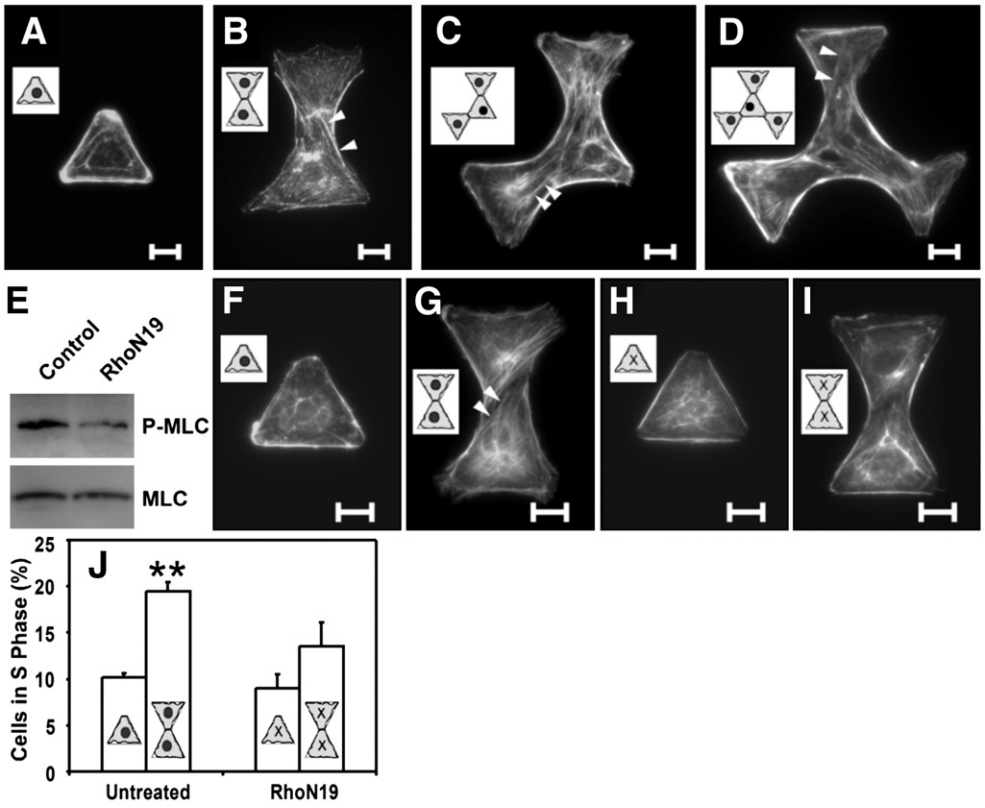

Fig. 3 – Changes in proliferation with cell–cell contact are mediated by the actin cytoskeleton and signaling through RhoA. (A–D Fluorescence images of actin stress fibers and inset illustrations of groups of BPAECs without (A) and with (B–D) cell–cell contact. (E) Western blots for dual-phosphorylated myosin light chain (P-MLC) and total myosin light chain (MLC) in control cells (left) or cells expressing RhoN19 (right). (F–I) Fluorescence images of actin stress fibers and inset illustrations of control cells (F, G) or cells expressing RhoN19 (H, I). These cells are either single (F, H) and paired (G, I). (J) Graph of BrdU incorporation in untransfected cells, and cells transfected with dominant negative RhoN19. Arrowheads in (B–D, G) indicate representative stress fibers, with two arrowheads pointing to one fiber. In inset illustrations of cell geometry, "X" indicates transfection with RhoN19. Error bars are standard error with (**) $p<0.001$ versus corresponding case of zero neighbors by *t*-test. Scale bars are 10 μm.

Intracellular, not intercellular, tension leads to proliferation increase

While blocking RhoA activity inhibited the proliferative response to cell–cell contact, it remained unclear whether cell–cell contact affected RhoA signaling or whether RhoA altered proliferation indirectly by affecting cell–cell junctions. To examine whether cell–cell junctions were disrupted by blocking RhoA activity, we compared junctional localization of β-catenin, a component of adherens junctions, in pairs of cells either expressing the dominant negative RhoA or not (Fig. 4D). While β-catenin stained diffusely with a faint nuclear localization in single cells, a bright band at the cell–cell junction indicated the formation of cadherin-mediated junctions in pairs of cells. Expression of RhoN19 in either singles or pairs did not affect β-catenin localization, suggesting that RhoA signaling is not a prerequisite for the formation or maintenance of cell–cell contacts, and that alteration of RhoA signaling in these experiments did not significantly interfere with cell–cell contacts. Therefore, the data support the hypothesis that cell–cell contacts signal through RhoA to influence proliferation.

The observation that stress fibers bridged across cell–cell junctions in untreated cells but not in RhoN19 expressing cells suggests that cytoskeletal tension transmitted across the cell–cell junction may be necessary for proliferative signaling. To determine whether such intercellular tension or only intracellular tension within a given cell was necessary to affect proliferation, we generated mixed pairs of cells, in which only one cell expressed RhoN19 while its neighbor remained untreated. We postulated that, in such a mixed pair, tension across the cell–cell junction would be eliminated. In such pairs, stress fibers increased in the untreated cells, but not in the RhoN19-expressing cells (Fig. 4A). Thus, in terms of cytoskeletal integrity, untreated cells in contact with RhoN19-expressing neighbors behaved much like untreated cells with untreated neighbors, and similarly RhoN19-expressing cells did not change their behavior based on the type of neighbor with which they were paired.

In these conditions, we found that proliferation of RhoN19-expressing cells in the mixed pairs was low, and similar to untreated or RhoN19-expressing single cells. In contrast, untreated cells in the mixed pairs proliferated at the same high rate as untreated pairs of cells (Fig. 4C). Together, these data suggest that cytoskeletal tension across the cell–cell junction is not required in order to mediate the cell–cell signal to stimulate proliferation. Rather, RhoA signaling appears to be downstream

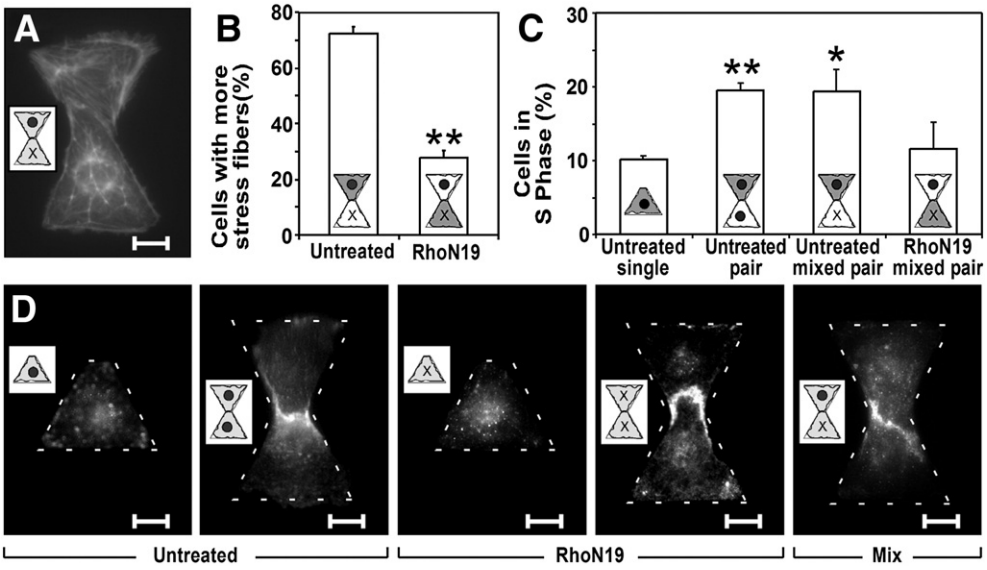

Fig. 4 – Increase in proliferation with cell–cell contact is mediated by intracellular, not intercellular, tension. (A) Fluorescence image of actin stress fibers and inset illustration of a "mixed" pair of cells containing an untreated cell (top) and a cell expressing RhoN19 (bottom). The "X" in the inset indicates expression of RhoN19. (B) Graph of the percentage of cells within mixed pairs that exhibited more stress fibers than their paired neighbor. Darker shading (inset illustrations) indicates the cell that was counted for each bar. (C) Graph of BrdU incorporation in single cells, in pairs of cells, and in mixed pairs of cells containing one untreated and one RhoN19 expressing cell. For mixed pairs, untreated and RhoN19 expressing cells were counted separately. Darker shading (inset illustrations) indicates the cell that was counted for each bar. (D) Immunofluorescence images of β-catenin in single and paired cells. As indicated, cells were either untreated, transfected with RhoN19, or mixed pairs containing one untreated and one RhoN19 expressing cell. In the mixed pair, the upper and lower cells are untreated and RhoN19 expressing, respectively. Dotted white lines indicate the borders of the wells. Error bars are standard error with (*) $p<0.05$ and (**) $p<0.001$ versus untreated control by *t*-test. Scale bars are 10 μm.

in the intracellular transmission of cell–cell signaling to proliferation. Therefore, we conclude that intracellular tension, and not tension across the cell–cell contact, is a necessary component of the cell–cell contact-induced proliferative response.

Engagement of VE-cadherin is sufficient for stimulation of proliferation

Although a compromised actin cytoskeleton indicated that tension-deficient cells expressing Ad-RhoN19 would be unable to apply tension to their neighbors, the possibility remained that untreated cells could apply tension to deficient neighbors, which would provide passive resistance. Moreover, it was unclear what surface receptors might be responsible for this proliferative effect. Previous studies in our laboratory have suggested that engagement of VE-cadherin stimulates proliferation through a RhoA-mediated signaling pathway. To explore whether engagement of VE-cadherin alone stimulates proliferation, we engaged the cadherins of single isolated, patterned BPAECs using a chimera of the ectodomain of human VE-cadherin fused to the immunoglobulin Fc domain (hVE-Fc) bound to protein-A-coated beads (Fig. 5A). We found that endothelial cells bound to hVE-Fc-coated beads exhibited higher proliferation when compared with cells without beads (Fig. 5B). These data demonstrate that the engagement of VE-cadherin alone stimulates proliferation and confirmed that tension transmitted across cell–cell junctions was not required for the increase in proliferation induced by cell–cell contact.

Discussion

Here, we were able to create defined multicellular aggregates by actively positioning each of the cells involved. In previous studies groups of cells could be randomly assembled [25], but with such

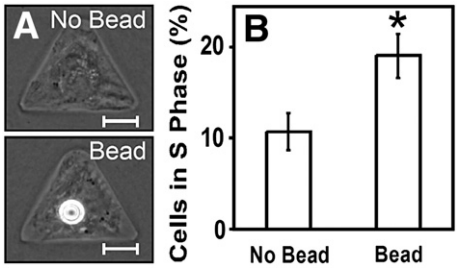

Fig. 5 – Proliferation in patterned cells increases upon contact with VE-cadherin-coated beads. (A) Phase contrast images of solitary spread cells without (top) and with (bottom) a VE-cadherin-coated bead. (B) Graph of BrdU incorporation in spread cells without and with a bead. Error bars are standard error, with (*) $p<0.05$ versus control by *t*-test. Scale bars are 10 μm.

techniques one could not simultaneously control the degree of cell spreading on substrates coated with ECM protein. With the advent of micropatterned surfaces, cell spreading could be controlled by plating single cells on ECM-coated islands of specified size, but this technique did not allow the control of cell–cell contact in groups of cells. Because multiple cells cultured on these islands could move freely, the number and size of their cell–cell contacts was neither predetermined nor static [4,18,26]. The use of micropatterned wells allowed for simultaneous control of cell–ECM contact and cell–cell adhesion, but only in pairs of cells [8,18]. Here, by embedding active trapping electrodes into the substrate, we facilitated rapid positioning of large numbers of cells into more complex multicellular groups to study the effects of cell–cell contact on proliferation in endothelial cells. The method itself is not limited to aggregates of one to four cells, or to endothelial cells [19]. In fact, multiple cell types could be positioned on the same substrate by selectively activating the electrical traps, such that heterogeneous multicellular organization could be defined with single cell precision.

The aggregates of endothelial cells in the current work, having predefined spreading, contact, and numbers of cells, allowed a well-controlled study of the response of proliferation in endothelial cells to cell–cell contact. Several previous studies have linked cell–cell contact and VE-cadherin to endothelial proliferation [7,8,15,18]. The widespread notion of contact inhibition of proliferation is derived from the classical observation that plating cells at higher density, and thus with more cell–cell contact, decreases proliferation. Yet, we previously showed that cell–cell contact with a single neighbor could stimulate proliferation. Using our new system to vary the number of cell–cell contacts while holding cell spreading constant, we showed that proliferation responds biphasically to cell–cell contact, suggesting one possible mechanism contributing to the two previously observed (stimulatory and inhibitory) proliferative responses.

A biphasic proliferative response may explain multiple facets of growth control in endothelial cells. Endothelial cells in the interior of a monolayer, where a high degree of cell–cell contact occurs, are prevented from proliferating by the classic model of contact inhibition. However, cells in the context of a wound edge may experience fewer contacts with neighbors and thereby experience "contact-stimulated" proliferation. As seen with the multicellular aggregates in the study, those cells at the edge of the group proliferated more than at the center. The changes we observed were moderate, but all cells, even those with three neighbors, had a significant amount of free edge, whereas endothelial cells within a monolayer would be completely surrounded by neighbors. It is indeed possible that the amount of cell–cell contact, and therefore the quantity of engaged cadherin molecules, may influence the levels of proliferation.

Our results agree with previous assertions that, although forces across adherens junctions are transduced into mechanical and biochemical signals [27], forces at these contacts do not translate directly into proliferative effects [28]. Rather, cell–cell contact appears to biochemically regulate RhoA signaling, which in turn may affect proliferation through multiple effectors [29,30]. Forces on focal adhesions between a cell and the ECM, on the other hand, have been shown in several studies to increase proliferation [31,32]. Therefore, despite their analogous nature, cell–cell and cell–ECM contact may regulate proliferation by differing mechanisms.

Several studies have begun to untangle the interwoven milieu of factors that drive proliferation. While soluble factors, cytoskeletal organization, mechanical forces, and cell–ECM have clearly defined roles in proliferative regulation, the influence of cell–cell contacts has been more difficult to interpret. Cell–cell contact involves multiple controls on proliferation that include cooperation with growth factor receptor signaling [13,16,33] and cell spreading [8]. It is perhaps these multiple crosstalk mechanisms that underlie the opposing stimulatory and inhibitory effects of cell–cell contact on proliferation (Fig. 6), and how various cell–cell juxtapositions may provide critical cues for restricting different cellular responses to appropriate spatial locations within a complex tissue.

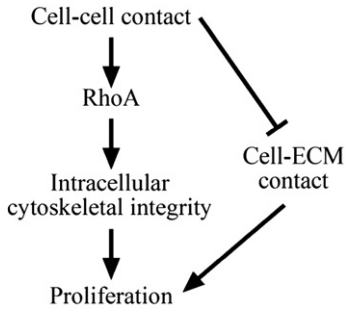

Fig. 6 – Model proposing how cell–cell contact might promote a biphasic proliferative response. Cell–cell contact stimulates the RhoA signaling pathway, which increases assembly of the actin cytoskeleton in individual cells, triggering increased proliferation. As cell–cell contact increases, the degree of cell contact with the extracellular matrix (ECM) may be decreased, thereby down-regulating proliferation.

Acknowledgments

We thank Susan Craig and Dana Pirone for invaluable guidance; and Elisabetta Dejana, Daniel Reich, Lewis Romer, Nathan Sniadecki, and Joel Voldman for helpful discussions. This work was supported in part by the NIH (HL 073305; EB00262), the Office of Naval Research, The Whitaker Foundation, and the Defense Advanced Projects Research Agency. DSG acknowledges financial support from The Whitaker Foundation and Medtronic, Inc. WFL acknowledges financial support from the NSF. CJS acknowledges financial support from the Paul and Daisy Soros Foundation. CMN acknowledges financial support from the Whitaker Foundation.

Appendix A. Supplementary data

Supplementary data associated with this article can be found, in the online version, at doi:10.1016/j.yexcr.2008.06.023.

REFERENCES

[1] B. Alberts, A. Johnson, J. Lewis, M. Raff, K. Roberts, P. Walter, Molecular Biology of the Cell, 4th ed., Garland, New York, 2002.
[2] S.M. Frisch, E. Ruoslahti, Integrins and anoikis, Curr. Opin. Cell. Biol. 9 (1997) 701–706.

[3] J. Folkman, A. Moscona, Role of cell shape in growth control, Nature 273 (1978) 345–349.
[4] C.S. Chen, M. Mrksich, S. Huang, G.M. Whitesides, D.E. Ingber, Geometric control of cell life and death, Science 276 (1997) 1425–1428.
[5] Q. Li, Y. Muragaki, H. Ueno, A. Ooshima, Stretch-induced proliferation of cultured vascular smooth muscle cells and a possible involvement of local renin–angiotensin system and platelet-derived growth factor (PDGF), Hypertens Res. 20 (1997) 217–223.
[6] M. Stula, H.D. Orzechowski, S. Gschwend, R. Vetter, R. von Harsdorf, R. Dietz, M. Paul, Influence of sustained mechanical stress on Egr-1 mRNA expression in cultured human endothelial cells, Mol. Cell. Biochem. 210 (2000) 101–108.
[7] L. Caveda, I. Martin-Padura, P. Navarro, F. Breviario, M. Corada, D. Gulino, M.G. Lampugnani, E. Dejana, Inhibition of cultured cell growth by vascular endothelial cadherin (cadherin-5/VE-cadherin), J. Clin. Invest. 98 (1996) 886–893.
[8] C.M. Nelson, C.S. Chen, VE-cadherin simultaneously stimulates and inhibits cell proliferation by altering cytoskeletal structure and tension, J. Cell. Sci. 116 (2003) 3571–3581.
[9] D.S. Ettenson, A.I. Gotlieb, Endothelial wounds with disruption in cell migration repair primarily by cell proliferation, Microvasc. Res. 48 (1994) 328–337.
[10] J. Folkman, Y. Shing, Angiogenesis, J. Biol. Chem. 267 (1992) 10931–10934.
[11] F. Fagotto, B.M. Gumbiner, Cell contact-dependent signaling, Dev. Biol. 180 (1996) 445–454.
[12] B.M. Gumbiner, Cell adhesion: the molecular basis of tissue architecture and morphogenesis, Cell 84 (1996) 345–357.
[13] P.A. Underwood, P.A. Bean, J.R. Gamble, Rate of endothelial expansion is controlled by cell:cell adhesion, Int. J. Biochem. Cell. Biol. 34 (2002) 55–69.
[14] A. Ferber, C. Yaen, E. Sarmiento, J. Martinez, An octapeptide in the juxtamembrane domain of VE-cadherin is important for p120ctn binding and cell proliferation, Exp. Cell. Res. 274 (2002) 35–44.
[15] M.A. Castilla, M.V. Arroyo, E. Aceituno, P. Aragoncillo, F.R. Gonzalez-Pacheco, E. Texeiro, R. Bragado, C. Caramelo, Disruption of cadherin-related junctions triggers autocrine expression of vascular endothelial growth factor in bovine aortic endothelial cells: effects on cell proliferation and death resistance, Circ. Res. 85 (1999) 1132–1138.
[16] M. Grazia Lampugnani, A. Zanetti, M. Corada, T. Takahashi, G. Balconi, F. Breviario, F. Orsenigo, A. Cattelino, R. Kemler, T.O. Daniel, E. Dejana, Contact inhibition of VEGF-induced proliferation requires vascular endothelial cadherin, beta-catenin, and the phosphatase DEP-1/CD148, J. Cell. Biol. 161 (2003) 793–804.
[17] D.M. Pirone, W.F. Liu, S.A. Ruiz, L. Gao, S. Raghavan, C.A. Lemmon, L.H. Romer, C.S. Chen, An inhibitory role for FAK in regulating proliferation: a link between limited adhesion and RhoA-ROCK signaling, J. Cell. Biol. 174 (2006) 277–288.
[18] C.M. Nelson, C.S. Chen, Cell–cell signaling by direct contact increases cell proliferation via a PI3K-dependent signal, FEBS Letters 514 (2002) 238–242.
[19] D.S. Gray, J.L. Tan, J. Voldman, C.S. Chen, Dielectrophoretic registration of living cells to a microelectrode array, Biosens. Bioelectron. 19 (2004) 771–780.
[20] A. Docoslis, N. Kalogerakis, L. Behie, Dielectrophoretic forces can be safely used to retain viable cells in perfusion cultures of animal cells, Cytotechnology 30 (1999) 133–142.
[21] T. Heida, W.L. Rutten, E. Marani, Dielectrophoretic trapping of dissociated fetal cortical rat neurons, IEEE Trans. Biomed. Eng. 48 (2001) 921–930.
[22] H. Glasser, G. Fuhr, Cultivation of cells under strong ac-electric field — differentiation between heating and trans-membrane potential effects, Bioelectro. Bioenerg. 47 (1998) 301–310.
[23] S. Archer, T.T. Li, A.T. Evans, S.T. Britland, H. Morgan, Cell reactions to dielectrophoretic manipulation, Biochem. Biophys. Res. Commun. 257 (1999) 687–698.
[24] J. Voldman, R.A. Braff, M. Toner, M.L. Gray, M.A. Schmidt, Holding forces of single-particle dielectrophoretic traps, Biophys. J. 80 (2001) 531–541.
[25] D.A. Wollner, K.A. Krzeminski, W.J. Nelson, Remodeling the cell surface distribution of membrane proteins during the development of epithelial cell polarity, J. Cell. Biol. 116 (1992) 889–899.
[26] C. Brangwynne, S. Huang, K.K. Parker, D.E. Ingber, E. Ostuni, Symmetry breaking in cultured mammalian cells, In Vitro Cell. Dev. Biol. Anim. 36 (2000) 563–565.
[27] A. Shay-Salit, M. Shushy, E. Wolfovitz, H. Yahav, F. Breviario, E. Dejana, N. Resnick, VEGF receptor 2 and the adherens junction as a mechanical transducer in vascular endothelial cells, PNAS 99 (2002) 9462–9467.
[28] M.A. Schwartz, M.H. Ginsberg, Networks and crosstalk: integrin signalling spreads, Nat. Cell. Biol. 4 (2002) E65–E68.
[29] A.B. Jaffe, A. Hall, Rho GTPases in transformation and metastasis, Adv. Cancer Res. 84 (2002) 57–80.
[30] K. Burridge, K. Wennerberg, Rho and Rac take center stage, Cell 116 (2004) 167–179.
[31] S. Huang, D.E. Ingber, The structural and mechanical complexity of cell-growth control, Nat. Cell. Biol. 1 (1999) E131–E138.
[32] M.A. Schwartz, R.K. Assoian, Integrins and cell proliferation: regulation of cyclin-dependent kinases via cytoplasmic signaling pathways, J. Cell. Sci. 114 (2001) 2553–2560.
[33] C.G. Kevil, D.K. Payne, E. Mire, J.S. Alexander, Vascular permeability factor/vascular endothelial cell growth factor-mediated permeability occurs through disorganization of endothelial junctional proteins, J. Biol. Chem. 273 (1998) 15099–15103.